

Chemical Science

Accepted Manuscript

This article can be cited before page numbers have been issued, to do this please use: X. Zhang, J. Leng, Q. Sun, Q. Dong, X. Tong, Y. Song, Y. Xu, S. Jin and W. Tian, *Chem. Sci.*, 2026, DOI: 10.1039/D6SC01780K.



This is an Accepted Manuscript, which has been through the Royal Society of Chemistry peer review process and has been accepted for publication.

Accepted Manuscripts are published online shortly after acceptance, before technical editing, formatting and proof reading. Using this free service, authors can make their results available to the community, in citable form, before we publish the edited article. We will replace this Accepted Manuscript with the edited and formatted Advance Article as soon as it is available.

You can find more information about Accepted Manuscripts in the [Information for Authors](#).

Please note that technical editing may introduce minor changes to the text and/or graphics, which may alter content. The journal's standard [Terms & Conditions](#) and the [Ethical guidelines](#) still apply. In no event shall the Royal Society of Chemistry be held responsible for any errors or omissions in this Accepted Manuscript or any consequences arising from the use of any information it contains.

ARTICLE

Slow Cooling and Efficient Extraction of Hot Carriers in Perovskite Films via Engineering Trap-Mediated Relaxation Channel

Xinlei Zhang,^{a,b} Jing Leng,^{*b} Qi Sun,^b Qingshun Dong,^b Xinyu Tong,^b Yu Song,^a Yan Xu,^{*a} Shengye Jin^{*b} and Wenming Tian^{*b}Received 00th January 20xx,
Accepted 00th January 20xx

DOI: 10.1039/x0xx00000x

Long-lived hot carriers (HCs) are highly desired for HC photovoltaics, but achieving slow HC relaxation is challenging because strong electron-phonon interaction typically drives rapid thermalization. Herein, we investigate the influence of excess PbI_2 on HC relaxation in formamidinium lead iodide (FAPbI₃) perovskite films using femtosecond transient absorption spectroscopy. Our results show that excess PbI_2 significantly slows down the HC relaxation at high excitation densities, extending their lifetime to hundreds of picoseconds. This effect arises from intraband trap states (ITS) introduced by excess PbI_2 , enabling an ITS-mediated channel that suppress direct HC relaxation under high densities due to hot phonon bottleneck. Owing to the remarkably suppressed HC relaxation, efficient HC extraction was successfully achieved in PbI_2 -rich perovskite films by incorporating electron acceptors. Our findings suggest an effective approach to prolong HC lifetime in perovskite films via engineering ITS, offering a valuable guideline for the rational design of high-efficiency HC photovoltaic devices.

Introduction

Due to the presence of the Shockley-Queisser (S-Q) limit, the power conversion efficiency (PCE) of single-junction solar cells is fundamentally constrained.¹⁻³ This limitation primarily results from the rapid dissipation of excess energy in the form of heat during carrier thermalization. To overcome this limit, the concept of hot-carrier solar cells has been proposed, aiming to extract hot carriers (HCs) before thermalization and achieve efficiencies beyond the S-Q limit.^{4, 5} Recently, lead halide perovskites have emerged as a promising candidate for solar energy conversion owing to their strong and broad absorption, large diffusion coefficient, long carrier lifetimes, and tunable bandgaps.⁶⁻¹¹ Especially, under high excitation densities, this class of materials exhibit significant hot phonon bottleneck (HPB) effect due to their large electron-phonon interaction, which greatly slows down HC relaxation process and thereby extends their lifetime to tens of ps.¹²⁻¹⁵ This feature enables perovskite materials to show great potential for efficient HC extraction, offering a new opportunity to break the S-Q limit for high-efficiency photovoltaic applications.

Recently, it has been discovered that incorporating polar cations into perovskite films can introduce new intraband intermediate states, thereby significantly slowing down HC relaxation process via altering their relaxation pathway, which

provides another effective way to extend the lifetime of HCs.¹⁶ As is well known, for perovskite solar cells with relatively high efficiency ($\geq 20\%$), excess PbI_2 is often found to aggregate at the grain boundaries and interfaces of perovskite films, indicating that residual PbI_2 might play an important role in affecting their carrier dynamics and device performance.¹⁷⁻¹⁹ Lots of experimental studies have confirmed that an appropriate excess of PbI_2 can passivate grain-boundary defects, improve crystallinity, and enhance device performance;^{20, 21} however, excessive PbI_2 may also lead to the increase of nonradiative recombination centres and the reduction of photovoltaic efficiency.²²⁻²⁴ Meanwhile, some theoretical studies have also shown that excess PbI_2 may easily lead to the formation of some defects, such as iodine vacancy and interstitial iodine, due to their low formation energies.^{25, 26} These defect levels are even found to be likely higher than conduct band minimum (CBM) or valent band maximum (VBM),²⁷ suggesting that excess PbI_2 might affect the lifetime of HCs by modifying their relaxation pathway. Although the impact of excess PbI_2 on defect formation and band-edge carrier kinetics in perovskite films, as well as their device performances, has been widely reported,²⁸⁻³⁰ it is still unclear how it influences the HC relaxation dynamics.

Formamidinium perovskite (FAPbI₃) has garnered broad attention due to its narrower bandgap and better stability.³¹⁻³⁴ Herein, we take FAPbI₃ films as an example to investigate the influence of excess PbI_2 on their HC relaxation by using femtosecond transient absorption (TA) spectroscopy. The results show that under high excitation intensities, the relaxation process of HCs in FAPbI₃ films with excess PbI_2 can be greatly slowed down, leading to their lifetime of up to hundreds of ps. It is because excess PbI_2 can introduce new intraband trap states (ITSs), thereby enabling an ITS-mediated HC relaxation pathway at high excitation density, which, however, is absent at low excitation density. This discrepancy is

^a Department of Chemistry, College of Sciences, Northeastern University, Shenyang 110819, China. E-mail: xuyan@mail.neu.edu.cn

^b State Key Laboratory of Chemical Reaction Dynamics, Dalian Institute of Chemical Physics, Chinese Academy of Sciences, Dalian 116023, China. E-mail: ljyx@dicp.ac.cn; sjin@dicp.ac.cn; tianwm@dicp.ac.cn

† Electronic Supplementary Information (ESI) available: Details about sample preparation and characterization, transient absorption measurements and other results of measurements See DOI: 10.1039/x0xx00000x



mainly a result of the competition between the direct and ITS-mediated relaxation channel of HCs under different densities. By incorporating appropriate acceptors, we successfully achieved the efficient extraction of HCs in FAPbI₃ films containing excess PbI₂ due to the prolonged HC lifetime. Our findings demonstrate a practical way to suppress HC relaxation in perovskite films via precise control of PbI₂ content, which might be of great significance for improving the performance of HC photovoltaic devices.

Results and discussion

In this work, in order to study the effect of excess PbI₂ on carrier dynamics in perovskite films, we prepared five batches of FAPbI₃ films with different PbI₂ contents using a previously reported two-step method,³⁵ in which the PbI₂ content was controlled by adjusting PbI₂ concentration in their precursors (more details about material preparation can be found in ESI). For convenience, these as-prepared perovskite films are denoted as FAPbI₃-x (i.e., FAPbI₃-1M, FAPbI₃-1.25M, FAPbI₃-1.5M, FAPbI₃-1.75M and FAPbI₃-2M) where x represents the PbI₂ concentration in their precursors. The representative SEM images of these samples are presented in Fig. S1, showing pronounced segregation along grain boundaries. As shown in Fig. 1a and S2, the UV-vis absorption spectra of these samples exhibit the same characteristic peaks at ~785 nm, while the peak positions of their photoluminescence (PL) spectra are located at ~803 nm, both consistent with previous reports.³⁶ The crystal structure and crystallinity of these films were further examined by X-ray diffraction (XRD). As shown in Fig. 1b, all as-prepared FAPbI₃ films display diffraction peaks at 14° and 28.1°, corresponding to the (100) and (200) planes of the α -phase FAPbI₃, respectively.^{37, 38} With the increase of PbI₂ content, another diffraction peak at 12.5° (corresponding to the (001) plane of PbI₂) begins to appear from PbI₂ concentration >1.5 M and its intensity gradually increases.³⁹ These observations strongly confirm the coexistence of perovskite and PbI₂ phases in these films and also demonstrate that PbI₂ contents in the films can be effectively tuned by controlling PbI₂ concentration in the precursors.

We first investigate the carrier dynamics in these samples under low excitation intensity by using femtosecond TA spectroscopy (see ESI for more details). Fig. 1c presents the representative two-dimensional (2D) pseudo-color TA maps of FAPbI₃-1.5M sample under 400 nm excitation with a low fluence of 0.1 $\mu\text{J}/\text{cm}^2$ and its corresponding TA spectra at different delays are shown in Fig. S3. The TA spectra exhibit a pronounced exciton bleaching (XB) peak centered at 793 nm,⁴⁰ consistent with its steady-state absorption spectrum (Fig. 1a). The XB signal originates from the state filling of band-edge carriers and thus its kinetics exactly represents the time evolution of band-edge carriers after photoexcitation.⁴¹ Fig. S4 plots the 2D pseudo-color TA images for other samples with different PbI₂ contents and their corresponding XB kinetics are also compared in Fig. 1d, showing similar spectral feature and kinetic behavior. These similar spectra, as well as their similar XRD patterns, between various samples indicate that excess PbI₂ hardly alters the bandgap and crystal structure of perovskite films. We note that the XB kinetics in all samples exhibit ultrafast rise (< 1 ps) (see the inset of Fig. 1d), indicating that their HCs undergo rapid relaxation to the band edge under low excitation intensity.

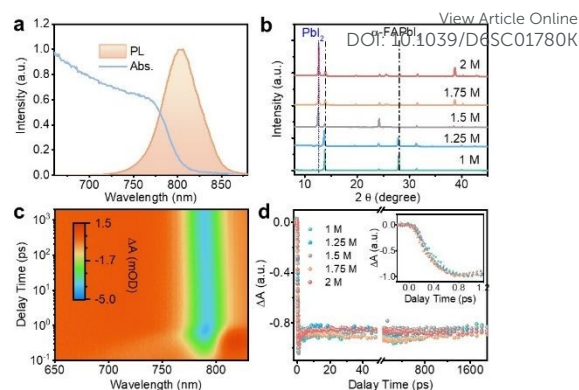


Fig. 1 Optical properties of FAPbI₃ films with different PbI₂ contents. (a) UV-vis absorption and PL spectra of FAPbI₃-1.5M. (b) XRD patterns of FAPbI₃ films with different PbI₂ contents. (c) 2D pseudo color image of TA spectra of FAPbI₃-1.5M under 400 nm excitation at a low fluence of 0.1 $\mu\text{J}/\text{cm}^2$. (d) Comparison of XB kinetics of five kinds of FAPbI₃ films under 400 nm excitation at a fluence of 0.1 $\mu\text{J}/\text{cm}^2$.

To study the effect of excess PbI₂ on HC relaxation, we next performed TA measurements on two typical FAPbI₃ films with different PbI₂ contents under 400 nm excitation with a high fluence of 33 $\mu\text{J}/\text{cm}^2$. Fig. 2a shows the 2D pseudo-color TA spectra of FAPbI₃-1M with the lowest PbI₂ content. Except for a similar XB peak, the TA spectra under high excitation fluence exhibit a distinct feature compared to the low-fluence case. The TA spectrum at early delays exhibits a broad bleach signal extending into the high-energy region (to ~630 nm) due to the rapid evolution of initial nonequilibrium carriers into a Fermi-Dirac distribution.^{42, 43} As delay time increases, this high-energy tail gradually narrows, which evolves over ~100 ps towards a symmetric XB peak centered at 783 nm (Fig. 2a), clearly reflecting the slowing down of HC relaxation process. The significantly slowed down HC relaxation under high excitation intensity has already been widely observed in many perovskite films,^{13, 15} which is attributable to the remarkable HPB effect at high carrier density. Fig. 2b presents the 2D pseudo-color TA image of FAPbI₃-1.5M. Similarly, the TA spectra at early delays also show obviously broadened bleach signal, indicating the presence of HPB in the sample. However, compared to FAPbI₃-1M, FAPbI₃-1.5M shows obviously narrower high-energy tails at initial delays (Fig. 2b and S5), suggesting the reduced HPB effect observed in the sample with excess PbI₂.

In order to further compare the HPB effect, we extracted the carrier temperature (T_c) in the two samples by fitting the high-energy tail of TA spectra using a modified Maxwell-Boltzmann distribution (see ESI for detailed description).³⁸ To ensure that HCs have reached a quasi-equilibrium temperature, the HC cooling kinetics was analyzed starting from 0.5 ps delay. Fig. 2c and 2d respectively compare the cooling curves of HCs in FAPbI₃-1M and FAPbI₃-1.5M under 400 nm excitation at two different excitation fluences. The insets show their TA spectral fitting at high fluence, while those for low fluence are shown in Fig. S6. At low excitation density, HCs undergo rapid relaxation and T_c drops to room temperature within 1 ps, consistent with the ultrafast rise kinetics of XB signal (see the insert of Fig. 1d), while under high excitation density, the HCs exhibit slower cooling rate, which even slows down to tens of ps especially at later delays. Such slow HC cooling at high density strongly confirms



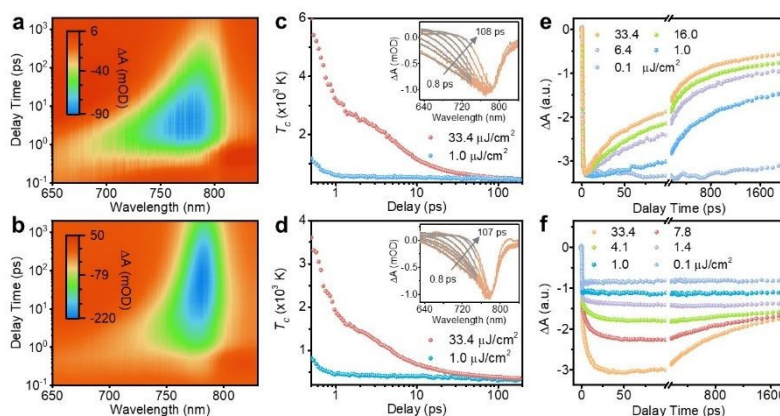


Fig. 2 Carrier dynamics of FAPbI₃-1M and FAPbI₃-1.5M. 2D pseudo color images of TA spectra under 400 nm excitation at 33.4 μJ/cm² for (a) FAPbI₃-1M and (b) FAPbI₃-1.5M. Temporal evolution of carrier temperature T_c of (c) FAPbI₃-1M and (d) FAPbI₃-1.5M under 400 nm excitation at indicated excitation fluences. The insets show their fitted high energy tails at higher fluence using Maxwell-Boltzmann distribution function. Comparison of XB kinetics normalized at 1 ps delay of (e) FAPbI₃-1M and (f) FAPbI₃-1.5M under indicated excitation intensities.

the presence of the HPB effect, which mainly originates from their large electron-phonon interaction, leading to the more rapid build-up of hot LO-phonon population and slower conversion rate from LO-phonons to acoustic phonons.^{13, 44} Compared with FAPbI₃-1M, the initial T_c value of FAPbI₃-1.5M is substantially lower, again confirming that the HPB effect is indeed reduced in FAPbI₃-1.5M film with higher PbI₂ content, consistent with the observed narrower high-energy tail in the sample (Fig. 2b).

Compared with FAPbI₃-1M, in addition to the reduced HPB effect, another more significant difference can be clearly observed in FAPbI₃-1.5M, where its XB signal still shows a remarkable growth trend within a hundred ps at high excitation density. To elucidate this strange behavior, we further examine the excitation-fluence dependence of XB kinetics in the two samples (Fig. 2e and 2f). Their pseudo-color TA maps under other excitation fluences are provided in Fig. S7 and S8. For FAPbI₃-1M film, although HC relaxation is remarkably slowed down at high excitation densities due to the HPB effect, its XB signal still reaches its maximum within a few ps due to the presence of stronger higher-order recombination, leading to its

faster decay rate at higher densities. In stark contrast, for FAPbI₃-1.5M, despite the weakened HPB effect, its XB signal rises very slowly and does not reach its maximum until ~ 100 ps under high excitation density (Fig. 2f), suggesting a slow HC relaxation process. A similar slow-rising XB kinetic behavior has recently been observed in mixed-cation FAPbI₃ films and was attributed to the HC relaxation mediated by a polar cation induced intraband intermediate state.¹⁶ However, unlike the above report, in which the slow-rising behavior also appeared at low excitation density, our observation occurs specifically in FAPbI₃-1.5M under high excitation fluence, and is absent in FAPbI₃-1M or at low fluences. This distinct dependence on composition and excitation intensity suggests that the underlying HC relaxation mechanism in our system may differ subtly from the one previously reported.

Recent reports confirm excess PbI₂ might create defect states higher than CBM or VBM.^{26, 27} In order to confirm this, we conducted first-principles density functional theory (DFT) calculations to explore the electronic states of iodine vacancies (V_I) and interstitial iodine (I_I) in FAPbI₃ perovskite films. The results indicate that iodine-related

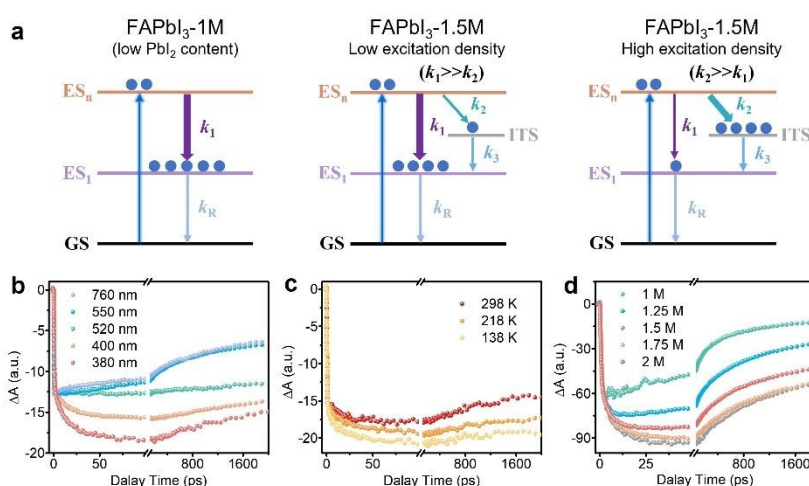


Fig. 3 Competition between direct and ITS-mediated HC relaxation pathways in FAPbI₃ films. (a) Schematic illustration of HC relaxation process. ES, excited state; ITS, intraband trap state; GS, ground state. (b) XB kinetics of FAPbI₃-1.5M under various excitation wavelengths with an initial carrier density of $\sim 3.3 \times 10^{18} \text{ cm}^{-3}$. (c) XB kinetics of FAPbI₃-1.5M under 400 nm excitation at a high fluence of 33.4 μJ/cm² at different temperatures. (d) XB kinetics in various FAPbI₃ films with different PbI₂ contents under 400 nm excitation at a fluence of 33.4 μJ/cm²



defects do introduce some localized electronic states above CBM (Fig. S9), confirming the existence of intraband trap state (ITS) induced by excess PbI_2 . To explain the slow rising behavior of XB signal in FAPbI_3 -1.5M, we presented a three-level kinetic model, in which the ITS above the lowest excited state (ES_1) is introduced to mediate HC relaxation (Fig. 3a). In FAPbI_3 -1M without ITS, the photogenerated HCs relax directly to ES_1 only via electron-phonon scattering, resulting in no slowly rising XB kinetics even at high densities. In contrast, in FAPbI_3 -1.5M with many ITSs, the photogenerated HCs may relax to ES_1 through two different channels: 1) directly relaxing to ES_1 via electron-phonon scattering at a rate of k_1 ; 2) first relaxing to ITS at a rate of k_2 and then transferring from ITS to ES_1 at a relatively slow rate of k_3 . At low excitation fluence, $k_1 \gg k_2$, resulting in inefficient ITS-mediated channel, and thus most carriers in FAPbI_3 -1.5M can directly relax rapidly to ES_1 , leading to the absence of slow rising component, similar to the case of FAPbI_3 -1M. However, at high densities, the presence of HPB can remarkably slow down the direct relaxation rate, resulting in $k_2 \gg k_1$, which leads to most carriers first relaxing to ITS and then transferring to ES_1 . Therefore, the slow-rising XB kinetics observed at high densities actually reflects the carrier transfer process from ITS to ES_1 .

To verify the above mechanism, we next performed an excitation-wavelength-dependent TA measurement under relatively high excitation fluences (Fig. 3b). Note that, for comparability, the excitation fluence at different wavelengths was adjusted to ensure the same initial carrier density ($\sim 3.3 \times 10^{18} \text{ cm}^{-3}$) generated in the sample. As expected, the slow-rising XB kinetics is only observed under short-wavelength excitation, while it disappears when the excitation wavelength exceeds 520 nm. This indicates that photogenerated carriers require sufficient energy to populate into ITS, confirming that the ITS level is higher than ES_1 . According to the excitation wavelength threshold, the ITS is estimated to be about 0.80 eV higher than ES_1 . To further understand the two relaxation channels, we conducted a temperature-dependent TA measurement under high excitation fluence (Fig. 3c). As the temperature increases, both the rise time and amplitude of the slow component increase,

suggesting a larger initial carrier population into ITS. Since the HPB effect becomes more severe at lower temperatures due to less efficient phonon scattering,¹⁴ the direct cooling channel will inevitably slow down, thereby enhancing the contribution from the ITS-mediated channel. These temperature-dependent results indicate that the slow-rising XB kinetics does stem from the ITS-mediated relaxation and can also be engineered by controlling the competition between the above two relaxation channels.

To further understand the role of excess PbI_2 , we examined the HC relaxation kinetics in more FAPbI_3 films with different PbI_2 contents under high excitation densities (Fig. S10). The comparison of their XB kinetics is shown in Fig. 3d. For FAPbI_3 -1M with the lowest PbI_2 content, its XB kinetics does not show the slow-rising component after 1 ps, suggesting the negligible formation of ITS likely due to insufficient PbI_2 . With the increase of PbI_2 concentration from 1.25 M to 1.5 M, the amplitude of the slow-rising XB kinetics in these samples does remarkably increase, strongly confirming the formation of more ITSs. This results in more carriers populating into ITS and thus less contribution from direct relaxation channel, leading to the weaker HPB observed in the samples with higher PbI_2 contents (Fig. 2a, 2b and S10). We also note that, when the PbI_2 concentration exceeds 1.5 M, the amplitude of the slow-rising component shows a slight decrease, which might be related to the weakening of HPB effect caused by material property. Compared with FAPbI_3 -1.5M, the films containing more PbI_2 exhibit smaller heat capacity (Fig. S11), which suggests faster heat conduction and weaker HPB effect, leading to faster direct relaxation and less population into ITS.

Slow cooling of HCs is highly desired for their effective extraction, but hard to realize because of the presence of strong electron-phonon interaction. Introducing an ITS via incorporating excess PbI_2 or other means might be an effective method to slow down the HC cooling and promote their extraction. To verify this idea, we fabricated three batches of FAPbI_3 -1.5M films via incorporating different electron acceptors, selected based on their band alignment with FAPbI_3 films (see ESI for detailed fabrication procedures).⁴⁵ Here two kinds of SnO_2 were prepared via different methods (i.e.,

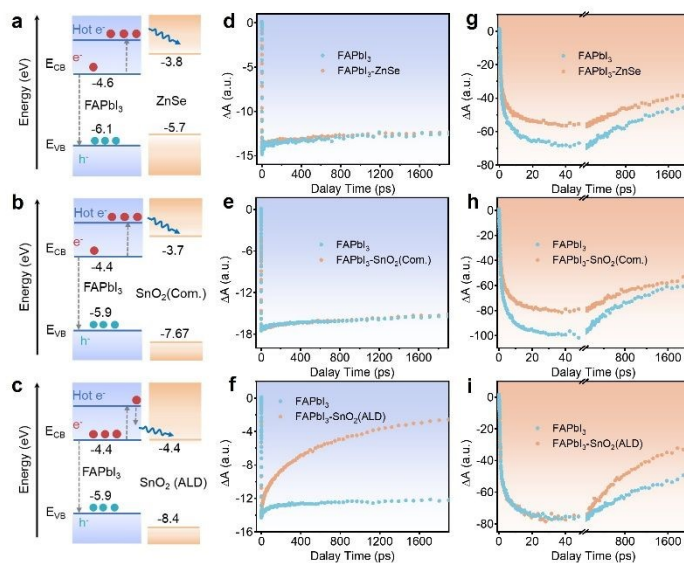


Fig. 4 Band alignment and HC extraction dynamics in FAPbI_3 films. (a-c) Energy level alignment of FAPbI_3 -1.5M interfaced with different electron acceptors: (a) ZnSe, (b) $\text{SnO}_2(\text{com.})$, and (c) $\text{SnO}_2(\text{ALD})$. (d-f) Comparison of XB kinetics in three sets of samples with and without (d) ZnSe, (e) $\text{SnO}_2(\text{com.})$ and (f) $\text{SnO}_2(\text{ALD})$ acceptor under near-bandgap excitation (760 nm, $2.7 \mu\text{J}/\text{cm}^2$). (g-i) Comparison of XB kinetics in three sets of samples with and without (g) ZnSe, (h) $\text{SnO}_2(\text{com.})$, and (i) $\text{SnO}_2(\text{ALD})$ acceptor under high-energy excitation (400 nm, $33.4 \mu\text{J}/\text{cm}^2$).



commercial and ALD-deposited), resulting in slightly different bandgaps and are labeled as SnO₂(Com.) and SnO₂(ALD), respectively. Fig. 4a-c show the band alignments of FAPbI₃ film and various acceptors, determined by ultraviolet photoelectron spectroscopy (Fig. S12 and S13). In principle, for ZnSe and SnO₂(Com.), due to their higher CBM levels than FAPbI₃, it is not possible to extract band-edge electrons, but it is possible to extract hot electrons, which is exactly opposite to SnO₂(ALD). Their abilities to extract band-edge carriers can also be directly reflected in the XB kinetic differences between the samples with and without acceptors under near-bandgap excitation at 760 nm (Fig. 4d-f). As expected, the dramatically faster recovery kinetics was observed in FAPbI₃-SnO₂(ALD) than in FAPbI₃, while for ZnSe and SnO₂(Com.), no difference in their XB kinetics was observed between the samples with and without acceptors. On this basis, we further compare the XB kinetics in the samples with and without acceptors under 400 nm excitation at a high fluence of 33.4 μJ/cm² (Fig. 4g-i). For the FAPbI₃-SnO₂(ALD) sample, no change was observed in the initial slow-rise kinetics (within 50 ps), suggesting that no hot electrons were extracted. In contrast, FAPbI₃-ZnSe and FAPbI₃-SnO₂(com.) exhibit a noticeable reduction in the amplitude of slow-rising component of XB kinetics, confirming that a fraction of hot electrons was successfully extracted into acceptors. These results strongly demonstrate the synergistic advantage of doping excess PbI₂ into perovskite films in conjunction with suitable electron acceptors, thereby retarding the HC relaxation and promoting their extraction. Based on this, we further fabricate two kinds of PSCs using FAPbI₃-1M and FAPbI₃-1.5M films and measure their J-V characteristics (Fig. S14). The results show the PSC with high PbI₂ content exhibits higher PCE and larger open-circuit voltage (V_{oc}) due to the excess energy of HC, demonstrating the positive role of HC extraction on PCE.

Conclusions

In summary, we have investigated the influence of excess PbI₂ on the HC relaxation process in FAPbI₃ perovskite films by using femtosecond TA spectroscopy. The results show that excess PbI₂ in FAPbI₃ films does significantly slow down the HC relaxation at high excitation density by introducing an ITS-mediated channel, leading to the occurrence of a slow-rising component (extending to hundreds of ps) in their XB kinetics. Through engineering the competition between the direct relaxation and ITS-mediated channel of HCs, this slow HC relaxation process can be controlled through adjusting the PbI₂ content, excitation density or temperature. Leveraging the prolonged HC lifetime, we successfully achieved the effective extraction of HCs in FAPbI₃ films containing excess PbI₂ by using an appropriate electron acceptor. Our findings suggest an effective method to slow down HC relaxation by creating ITS, which might be beneficial for the development of next-generation HC devices.

Author Contributions

W. T., J. L., Y. X. and S. J. conceived the project. X. Z. performed the sample preparation and characterization measurements, X. Z. conducted TA experiments with the assistance of X. T., X. Z. carried

out the electron acceptor tests with the help of Q. S. and Q. D. Y. S. conducted DFT calculations. The manuscript was drafted by X. Z. and revised by J. L., Y. X., S. J. and W. T. All the authors discussed the results and contributed to the manuscript.

Conflicts of interest

There are no conflicts to declare.

Data availability

The data supporting this article have been included as part of the supplementary information (SI). Supplementary information: Experimental details about sample preparation and TA measurement, additional TA data and other characterization results.

Acknowledgements

This work was supported by the Strategic Priority Research Program of the Chinese Academy of Sciences (XDB0970302), the National Natural Science Foundation of China (22233005, 22439001, 22171040), the CAS projects for Young Scientists in Basic Research (YSBR-007), the Natural Science Foundation of Liaoning (2024JH3/50100010), the Dalian Science and Technology Innovation Fund (2024RJ006), the DICP funding (DICP I202315) and Shenyang Young and Middle-aged Science and Technology Innovation Talent Support Program, China (No. RC230784).

Notes and references

- J. M. Ball and A. Petrozza, Defects in perovskite-halides and their effects in solar cells, *Nat. Energy*, 2016, **1**, 1-13.
- M. Lee Michael, J. Teuscher, T. Miyasaka, T. N. Murakami and H. J. Snaith, Efficient Hybrid Solar Cells Based on Meso-Structured Organometal Halide Perovskites, *Science*, 2012, **338**, 643-647.
- J.-P. Correa-Baena, M. Saliba, T. Buonassisi, M. Grätzel, A. Abate, W. Tress and A. Hagfeldt, Promises and challenges of perovskite solar cells, *Science*, 2017, **358**, 739-744.
- A. J. Nozik, Utilizing hot electrons, *Nat. Energy*, 2018, **3**, 170-171.
- A. P. Kirk and M. V. Fischetti, Fundamental limitations of hot-carrier solar cells, *Phys. Rev. B*, 2012, **86**, 165206.
- J. Jeong, M. Kim, J. Seo, H. Lu, P. Ahlawat, A. Mishra, Y. Yang, M. A. Hope, F. T. Eickemeyer, M. Kim, Y. J. Yoon, I. W. Choi, B. P. Darwich, S. J. Choi, Y. Jo, J. H. Lee, B. Walker, S. M. Zakeeruddin, L. Emsley, U. Rothlisberger, A. Hagfeldt, D. S. Kim, M. Grätzel and J. Y. Kim, Pseudo-halide anion engineering for α-FAPbI₃ perovskite solar cells, *Nature*, 2021, **592**, 381-385.
- J. Chen, M. E. Messing, K. Zheng and T. Pullerits, Cation-Dependent Hot Carrier Cooling in Halide Perovskite Nanocrystals, *J. Am. Chem. Soc.*, 2019, **141**, 3532-3540.
- S. Sien Lim, D. Giovanni, Q. Zhang, A. Solanki, N. F. Jamaludin, J. W. Melvin Lim, N. Mathews, S. Mhaisalkar, M. S. Pshenichnikov and T. C. Sum, Hot carrier extraction in CH₃NH₃PbI₃ unveiled by pump-push-probe spectroscopy, *Sci. Adv.*, 2019, **5**, 3620.
- J. Yin, R. Naphade, P. Maity, L. Gutiérrez-Arzaluz, D. Almalawi, I.



- S. Roqan, J.-L. Brédas, O. M. Bakr and O. F. Mohammed, Manipulation of hot carrier cooling dynamics in two-dimensional Dion-Jacobson hybrid perovskites via Rashba band splitting, *Nat. Commun.*, 2021, **12**, 3995.
- 10 P. Moazzezi, V. Yeddu, I. T. Cheong, M. R. Kokaba, S. Dayneko, Y. Ahmed and M. I. Saidaminov, Discovery of Perovskite Cosolvency and Undoped FAPbI₃ Single-Crystal Solar Cells Fabricated in Ambient Air, *J. Am. Chem. Soc.*, 2025, **147**, 10203-10211.
- 11 M. Geng, J. Li, K. Wang, L. Jiang, D. Lu, S. Iqbal, Y. Gu, L. Chen and T. Xu, Multiple functional bulk passivator pyrimidine derivative stabilizing perovskite precursors for efficient carbon-based perovskite solar cells, *Chem. Sci.*, 2025, **16**, 19317-19327.
- 12 H. Li, Q. Wang, Y. Oteki, C. Ding, D. Liu, Y. Guo, Y. Li, Y. Wei, D. Wang, Y. Yang, T. Masuda, M. Chen, Z. Zhang, T. Sogabe, S. Hayase, Y. Okada, S. Iikubo and Q. Shen, Enhanced Hot-Phonon Bottleneck Effect on Slowing Hot Carrier Cooling in Metal Halide Perovskite Quantum Dots with Alloyed A-Site, *Adv. Mater.*, 2023, **35**, 2301834.
- 13 Y. Yang, D. P. Ostrowski, R. M. France, K. Zhu, J. van de Lagemaat, J. M. Luther and M. C. Beard, Observation of a hot-phonon bottleneck in lead-iodide perovskites, *Nat. Photonics* 2015, **10**, 53-59.
- 14 X. Yu, P. Shi, S. Gong, Y. Huang, J. Xue, R. Wang and X. Chen, Modulating hot carrier cooling and extraction with A-site organic cations in perovskites, *J. Chem. Phys.*, 2024, **160**, 121102.
- 15 J. Fu, Q. Xu, G. Han, B. Wu, C. H. A. Huan, M. L. Leek and T. C. Sum, Hot carrier cooling mechanisms in halide perovskites, *Nat. Commun.*, 2017, **8**, 1-9.
- 16 C. Wang, W. Chu, F. Ye, Z. Ou, Z. Li, Q. Guo, Z. Zheng, Z. Wang, X. Liu, G. Fang, O. Prezhdo, T. Wang and H. Xu, Polar methylammonium organic cations detune state coupling and extend hot-carrier lifetime in lead halide perovskites, *Chem*, 2022, **8**, 3051-3063.
- 17 B.-w. Park, N. Kedem, M. Kulbak, D. Y. Lee, W. S. Yang, N. J. Jeon, J. Seo, G. Kim, K. J. Kim, T. J. Shin, G. Hodes, D. Cahen and S. I. Seok, Understanding how excess lead iodide precursor improves halide perovskite solar cell performance, *Nat. Commun.*, 2018, **9**, 3301.
- 18 W. Shao, H. Wang, F. Ye, C. Wang, C. Wang, H. Cui, K. Dong, Y. Ge, T. Wang, W. Ke and G. Fang, Modulation of nucleation and crystallization in Pbl₂ films promoting preferential perovskite orientation growth for efficient solar cells, *Energy Environ. Sci.*, 2023, **16**, 252-264.
- 19 D. Zhang, H. Zhang, H. Guo, F. Ye, S. Liu and Y. Wu, Stable α -FAPbI₃ in Inverted Perovskite Solar Cells with Efficiency Exceeding 22% via a Self-Passivation Strategy, *Adv. Funct. Mater.*, 2022, **32**, 2200174.
- 20 C. Luo, Y. Zhao, X. Wang, F. Gao and Q. Zhao, Self-Induced Type-I Band Alignment at Surface Grain Boundaries for Highly Efficient and Stable Perovskite Solar Cells, *Adv. Mater.*, 2021, **33**, 2103231.
- 21 Y. Gao, H. Raza, Z. Zhang, W. Chen and Z. Liu, Rethinking the Role of Excess/Residual Lead Iodide in Perovskite Solar Cells, *Adv. Funct. Mater.*, 2023, **33**, 2215171.
- 22 Z. Liu, P. Liu, M. Li, T. He, T. Liu, L. Yu and M. Yuan, Efficient and Stable FA-Rich Perovskite Photovoltaics: From Material Properties to Device Optimization, *Adv. Energy Mater.*, 2022, **12**, 2200111.
- 23 T. J. Jacobsson, J.-P. Correa-Baena, E. Halvani Anaraki, B. Philippe, S. D. Stranks, M. E. F. Bouduban, W. Tress, K. Schenk, J. Teuscher, J.-E. Moser, H. Rensmo and A. Hagfeldt, Unreacted Pbl₂ as a Double-Edged Sword for Enhancing the Performance of Perovskite Solar Cells, *J. Am. Chem. Soc.*, 2016, **138**, 10331-10343.
- 24 Q. Jiang, Z. Chu, P. Wang, X. Yang, H. Liu, Y. Wang, Z. Yin, D. Wu, X. Zhang and J. You, Planar-Structure Perovskite Solar Cells with Efficiency beyond 21%, *Adv. Mater.*, 2017, **29**, 1703852.
- 25 S. Shin, P. Nandi, S. Seo, H. S. Jung, N. G. Park and H. Shin, Enhancing Stability of Efficient Perovskite Solar Cells (PCE \approx 24.5%) by Suppressing Pbl₂ Inclusion Formation, *Adv. Funct. Mater.*, 2023, **33**.
- 26 H. Chen, H. Yan and Y. Cai, Effects of Defect on Work Function and Energy Alignment of Pbl₂: Implications for Solar Cell Applications, *Chem. Mater.*, 2022, **34**, 1020-1029.
- 27 F. Ren, H. Xiang, K. Zhao and C. Liu, Impacts of Pbl₂ on high-efficiency perovskite solar cells: exploring intercalation orientations and defects, *J. Mater. Chem. C*, 2023, **11**, 13281-13289.
- 28 C.-J. Tong, L. Li, L.-M. Liu and O. V. Prezhdo, Long Carrier Lifetimes in Pbl₂-Rich Perovskites Rationalized by Ab Initio Nonadiabatic Molecular Dynamics, *ACS Energy Lett.*, 2018, **3**, 1868-1874.
- 29 Y. Chen, Q. Meng, Y. Xiao, X. Zhang, J. Sun, C. B. Han, H. Gao, Y. Zhang, Y. Lu and H. Yan, Mechanism of Pbl₂ in Situ Passivated Perovskite Films for Enhancing the Performance of Perovskite Solar Cells, *ACS Appl. Mat. Interfaces* 2019, **11**, 44101-44108.
- 30 H. Y. Wang, M. Y. Hao, J. Han, M. Yu, Y. Qin, P. Zhang, Z. X. Guo, X. C. Ai and J. P. Zhang, Adverse Effects of Excess Residual Pbl₂ on Photovoltaic Performance, Charge Separation, and Trap-State Properties in Mesoporous Structured Perovskite Solar Cells, *Chem. Eur. J.*, 2017, **23**, 3986-3992.
- 31 A. D. Wright, C. Verdi, R. L. Milot, G. E. Eperon, M. A. Pérez-Osorio, H. J. Snaith, F. Giustino, M. B. Johnston and L. M. Herz, Electron-phonon coupling in hybrid lead halide perovskites, *Nat. Commun.*, 2016, **7**, 11755
- 32 G. Kim, H. Min, K. S. Lee, D. Y. Lee, S. M. Yoon and S. I. Seok, Impact of strain relaxation on performance of α -formamidinium lead iodide perovskite solar cells, *science*, 2020, **370**, 108-112.
- 33 H. Min, M. Kim, S.-U. Lee, H. Kim, G. Kim, K. Choi, J. H. Lee and S. I. Seok, Efficient, stable solar cells by using inherent bandgap of α -phase formamidinium lead iodide, *science*, 2019, **366**, 749-753
- 34 Z. Zheng, S. Wang, Y. Hu, Y. Rong, A. Mei and H. Han, Development of formamidinium lead iodide-based perovskite solar cells: efficiency and stability, *Chem. Sci.*, 2022, **13**, 2167-2183.
- 35 W. Hui, L. Chao, H. Lu, F. Xia, H. Wei, Z. Su, C. Niu, W. Tao, B. Du, D. Li, Y. Wang, H. Dong, S. Zuo, B. Li, W. Shi, X. Ran, P. Li, H. Zhang, Z. Wu, C. Ran, L. Song, G. Xing, X. Gao, J. Zhang, Y. Xia, Y. Chen and W. Huang, Stabilizing black-phase formamidinium perovskite formation at room temperature and high humidity, *Science*, 2021, **371**, 1359-1364.
- 36 S. Wang, Z. Miao, J. Yang, Z. Gu, P. Li, Y. Zhang and Y. Song, Lead-Chelating Intermediate for Air-Processed Phase-Pure FAPbI₃ Perovskite Solar Cells, *Angew. Chem. Int. Ed.*, 2024, **63**, e202407192.
- 37 Y. Zhang, T. Yang, S.-U. Lee, S. Liu, K. Zhao and N.-G. Park, Stabilizing α -Phase FAPbI₃ Perovskite Induced by an Ordered Solvated Quasi-Crystalline Pbl₂, *ACS Energy Lett.*, 2023, **9**, 159-167.
- 38 Y. Zhang, Y. Li, L. Zhang, H. Hu, Z. Tang, B. Xu and N. G. Park, Propylammonium Chloride Additive for Efficient and Stable FAPbI₃ Perovskite Solar Cells, *Advanced Energy Materials*, 2021, **11**, 2102538.
- 39 T. Yan, C. Zhang, S. Li, Y. Wu, Q. Sun, Y. Cui and Y. Hao, Multifunctional Aminoglycoside Antibiotics Modified SnO₂ Enabling High Efficiency and Mechanical Stability Perovskite

View Article Online

DOI: 10.1039/C4CY01700A

This journal is © The Royal Society of Chemistry 20xx

Open Access Article. Published on 07 May 2026. Downloaded on 5/8/2026 5:08:22 PM. This article is licensed under a Creative Commons Attribution-NonCommercial 3.0 Unported Licence.



- Solar Cells, *Adv. Funct. Mater.*, 2023, **33**, 2302336.
- 40 J. Yang, X. Wen, H. Xia, R. Sheng, Q. Ma, J. Kim, P. Tapping, T. Harada, T. W. Kee, F. Huang, Y.-B. Cheng, M. Green, A. Ho-Baillie, S. Huang, S. Shrestha, R. Patterson and G. Conibeer, Acoustic-optical phonon up-conversion and hot-phonon bottleneck in lead-halide perovskites, *Nat. Commun.*, 2017, **8**, 14120.
- 41 S. Wang, J. Leng, Y. Yin, J. Liu, K. Wu and S. Jin, Ultrafast Dopant-Induced Exciton Auger-like Recombination in Mn-Doped Perovskite Nanocrystals, *ACS Energy Lett.*, 2020, **5**, 328-334.
- 42 R. Zhang, Z. Zhou, X. Li, T. Pang, T. Song, H. Wu, Q. Liao, Z. Wang, F. Huang, K. Wu and D. Chen, Low-Threshold and Ultrastable Amplified Spontaneous Emission from CsPbBr₃@Glass via Glass Network Modulation, *ACS Nano*, 2025, **19**, 14318-14329.
- 43 S. Zheng, Q. Huang, W. Niu, R. Chen, T. Pang, L. Zeng and D. Chen, Tailoring Carrier Dynamics by Band Alignment Engineering in Quasi-2D Perovskite LED, *Nano Lett.*, 2025, **25**, 15927-15936.
- 44 M. B. Price, J. Butkus, T. C. Jellicoe, A. Sadhanala, A. Briane, J. E. Halpert, K. Broch, J. M. Hodgkiss, R. H. Friend and F. Deschler, Hot-carrier cooling and photoinduced refractive index changes in organic-inorganic lead halide perovskites, *Nat. Commun.*, 2015, **6**, 8420.
- 45 Y. Chen, Y. Lei, Y. Li, Y. Yu, J. Cai, M.-H. Chiu, R. Rao, Y. Gu, C. Wang, W. Choi, H. Hu, C. Wang, Y. Li, J. Song, J. Zhang, B. Qi, M. Lin, Z. Zhang, A. E. Islam, B. Maruyama, S. Dayeh, L.-J. Li, K. Yang, Y.-H. Lo and S. Xu, Strain engineering and epitaxial stabilization of halide perovskites, *Nature*, 2020, **577**, 209-215.

View Article Online
DOI: 10.1039/D6SC01780K

Open Access Article. Published on 07 May 2026. Downloaded on 5/8/2026 5:08:22 PM.
This article is licensed under a Creative Commons Attribution-NonCommercial 3.0 Unported Licence.



Data availability

The data supporting this article have been included as part of the supplementary information (SI).

Supplementary information: Experimental details about sample preparation and TA measurement, additional TA data and other characterization results.

